



## Detailed analysis of phase distributions in a vertical riser using wire mesh sensor (WMS)



M. Abdulkadir<sup>a,b,\*</sup>, V. Hernandez-Perez<sup>c</sup>, I.S. Lowndes<sup>c</sup>, B.J. Azzopardi<sup>c</sup>, E.T. Brantson<sup>b</sup>

<sup>a</sup> Department of Chemical Engineering, Federal University of Technology, Minna, Niger State, Nigeria

<sup>b</sup> Department of Petroleum Engineering, African University of Science and Technology, Abuja, Nigeria

<sup>c</sup> Process and Environmental Engineering Research Division, Faculty of Engineering, University of Nottingham, University Park, Nottingham NG7 2RD, United Kingdom

### ARTICLE INFO

#### Article history:

Received 19 February 2014

Received in revised form 22 July 2014

Accepted 22 July 2014

Available online 1 August 2014

#### Keywords:

Air–silicone oil

Air–water

WMS

Radial void fraction

Riser

### ABSTRACT

This paper looks into the results of an experimental study concerned with the phase distributions of gas–liquid multiphase flows experienced in a vertical riser. Scale experiments were carried out using a mixture of air and silicone oil in a 6 m long riser pipe with an internal diameter pipe of 67 mm. A series of pipe flow experiments were performed for a range of injected air superficial velocities over the range 0.05–4.73 m/s, whilst the liquid superficial velocities ranged from 0.05 to 0.38 m/s. Measurements of cross-sectional void fraction and radial time averaged void fraction across a pipe section located 4.92 m from the pipe flow injection were obtained using a capacitance wire mesh sensor (WMS). The data were recorded at a frequency of 1000 Hz over an interval of 60 s. For the range of flow conditions studied, the average void fraction was observed to vary between 0.1 and 0.83. An analysis of the data collected concluded that the observed void fraction was strongly affected by the gas superficial velocity, whereby the higher the gas superficial velocity, the higher was the observed average void fraction. The average void fraction distributions observed were in good agreement with the results obtained by other researchers. The accuracy and performance of void fraction correlations were carried out in terms of percentage error and Root Mean Square (RMS) error. Reasonably symmetric radial void fraction profiles were obtained when the air–silicone oil was fully developed, and the shape of the symmetry profile was strongly dependent on the gas superficial velocity. The data for air/water and air/silicone oil systems showed reasonably good agreement except at gas superficial velocity of 0.05 m/s. A comparison of the experimental data was performed against a published model to investigate the flow structure of air–water mixtures in a bubble column. A satisfactory report was observed for radial void fraction profile (mean relative error is within 5.7%) at the higher gas superficial velocities.

© 2014 Elsevier Inc. All rights reserved.

### 1. Introduction

Gas–liquid flow is ubiquitous and an extremely complicated physical phenomenon occurring particularly in the petroleum industry during the production and transportation of oil and gas due to its unsteady nature and high attendant pressure drop. The most common and safest means of transporting oil and gas from the sand face of wells to consumers is through pipelines. Pipelines used to transport fluids from the wellhead through different production facilities takes into consideration the pressure gradient along the pipelines. The spatial distribution of the phases inside the pipe and the pipe geometry plays an extremely important role

in the accurate determination of pressure gradient and flow hydrodynamic characteristics.

A vital characteristic of two-phase flow is the presence of moving interfaces and the turbulent nature of the flow that make theoretical predictions of flow parameters greatly more difficult than in single-phase flow. Thus, experimental measurements play an important role in providing information for design, and supporting analysis of system behavior. Because of this, there is a real need to make certain measurements of void fraction distribution for model development and testing. As it happens, these quantities must also be measured for control and monitoring of industrial two-phase systems. Void fraction is an important variable in any two-phase flow system for determining pressure loss, liquid holdup, and prediction of heat transfer. However, several studies concerning void fraction distribution have been carried out in vertical pipes (Abdulkadir et al. [1], Azzopardi et al. [2], [3–7],

\* Corresponding author.

E-mail address: [mukhau@futminna.edu.ng](mailto:mukhau@futminna.edu.ng) (M. Abdulkadir).

and Szalinski et al. [8]). In addition, several empirical and mechanistic correlations have been proposed in the literature using air/water as the operating fluid. Hence, engineers are often confronted with plethora of correlations to choose from for predicting void fraction. In addition, most of the reported works were confined to pipes with small internal diameters. But, only few studies have been published for void fraction distribution analysis in vertical pipes using more viscous fluid other than water [1,8].

Investigations by Harms and Forrest [9] and Jones [10] revealed that there are problems associated with inaccuracies in obtaining void fraction measurements owing to fluctuations.

## 1.1. Background to the study

### 1.1.1. Cross-sectional void fraction distribution

A critical literature review on cross-sectional void fraction distribution was included in Abdulkadir et al. [1]. In this section the summary is included. Gardner and Neller [11] conducted an experimental study to investigate the distribution and redistribution of the multiphase flow phenomena observed in air–water flow systems. They used a traversing probe to measure the time averaged void fraction at any point over a range of chosen cross-sections. They concluded that reasonably symmetric air concentration profiles were obtained at a distance of 3.3 m from the mixing section. However, they did not investigate the influence of gas superficial velocity on flow development and symmetry.

Morooka et al. [3] carried out a detailed measurement of void fraction of a vertical ( $4 \times 4$ ) rod bundle in a steam–water two-phase flow using an X-ray computing tomography (CT) scanner. They found that the cross-sectional averaged void fraction data for a bundle can be correlated by the Drift-Flux model and that the Zuber–Findlay correlation underestimated the data in a void fraction area of 80% or more. Based on this finding, they developed a modified correlation based on their data.

Ohnuki and Akimoto [12] studied the effect of air injection methods on the development of air–water two-phase flow along a 0.48 m internal diameter and 2.016 m height vertical pipe. The two injection methods, porous sinter and nozzle injection, were used to obtain different flow structures in the developing region. From an analysis of their experimental data they found that no air slugs occupying the flow path were recognized regardless of the air injection methods even under the condition where slug flow is realized in the small-scale pipe. They concluded that the lower half of the test section was affected by the air injection method, whilst for the upper half of the test section, the effects of the air injection methods observed were small.

Later, Ohnuki and Akimoto [4] extended their earlier work to studying the transition of flow pattern and phase distributions in the upward air–water flow observed along a 0.2 m internal diameter and 12.3 m height vertical pipe. They observed flow patterns and recorded measurements of axial differential pressure, phase distribution, bubble size and bubble and water velocities. They compared the data of other workers with their experimental data. They concluded that further detailed measurements were needed to investigate the flow structure under the agitated bubbly flow.

Prasser et al. [5] carried out detailed study of the evolution of flow structure with growing distance from the gas injection using a WMS. They carried out measurements in a vertical 51.2 mm internal diameter pipe using air–water as the working fluid at atmospheric pressure and a temperature of 30 °C. They found that the bubble size distributions clearly showed the effect of coalescence and fragmentation.

Shen et al. [7] studied two-phase distribution in a vertical 0.2 m internal diameter and a 24 m high pipe. They used optical probes and pressure transducers to record local measurements including; void fraction, Sauter mean diameter and pressure loss. From an

analysis of their experimental data they concluded that the phase distribution patterns could be subdivided into basic patterns, namely, wall peak and core peak using the concept of Fisher skewness. However, the weakness of Fisher skewness is its sensitivity to irregular observations at the extremes where the difference between the mean and the value is cubed.

Prasser et al. [6] carried out a detailed comparison of data obtained from an ultra-fast X-ray CT and a WMS. The work was carried out in a vertical 42 mm internal diameter pipe using air–water as the operating fluid. They found that the WMS has a significant higher resolution than the X-ray CT and that unlike the CT images; the WMS was capable of capturing small bubbles. They claimed that the WMS underestimated the gas fraction inside large bubbles. They concluded that the WMS caused a significant distortion to large Taylor bubbles for small liquid velocities up to 0.24 m/s and that this effect vanished with an increase in superficial water velocity.

Azzopardi et al. [2] carried out wire mesh sensor studies in a vertical 67 mm internal diameter pipe using air–water as the operating fluids. Measurements of radial time averaged void fraction and cross-sectional average time series of void fraction were carried out. They determined that the wire mesh sensor was capable of providing insight into the details of phase distributions in a pipe. The cross-sectional time averaged air void fraction was expressed in terms of the gas mass fraction. Also, these studies were restricted to the use of air–water flow mixtures.

Manera et al. [13] compared wire mesh sensor and conductive needle-probe measurements of vertical two-phase flow parameters using an air–water system. They determined that the WMS is capable of delivering a full mapping of the interfacial area density and a full three-dimensional reconstruction of gas bubbles. However, the needle probe was found to be less intrusive and produced fewer disturbances to the downstream flow.

Szalinski et al. [8] used a conductivity measuring WMS for air/water flow and a permittivity measuring one for air–silicone oil flows. The experiment was conducted in a 67 mm internal diameter and 6 m long vertical pipe. They made a direct comparison between both types of two-phase flow for the given pipe geometry and volumetric flow rates. Time series of cross-sectionally averaged void fraction was used to determine characteristics in amplitude and frequency space. They also used radial gas volume fraction profiles and bubble size distributions to compare air–water and air–silicone oil flows. The information from the time series and bubble size distribution was used to identify flow patterns for each of the flow rates studied.

Abdulkadir et al. [1] carried out an experimental investigation to characterize the phase distributions of two-phase air–silicone oil flow in a vertical pipe using WMS. This study concluded that reasonably symmetric profiles were obtained when the air–silicone oil was fully developed and that the shape of the profile was strongly dependent on the gas superficial velocity. They also determined that symmetric parabolic profiles can be represented as spherical cap bubble and slug flows and that flattened symmetric profile can be represented as churn flow. This paper is a follow-up of the work of [1]. Here, we present a detailed evaluation of the void fraction profile equations and comparison of air–silicone oil with other fluid systems.

### 1.1.2. Radial void fraction distribution

In two-phase gas–liquid flow, the local void fraction and local velocity vary across the pipe cross section. A modelling approach that takes into account this behavior is that called Drift Flux model. Here, the main assumption is that the velocity difference is due to the drift velocity between the phases. This approach, however, relies on several empirical parameters, such as the distribution parameter  $C_0$ . Analysis presented in Wallis [14] shows that  $C_0$

depends on the profiles of velocity and void fraction. As a result, efforts have been made to determine these profiles, in particular for the void fraction. In this sense, experimental measurements are of paramount importance.

The early work of Nassos and Bankoff [15] studied the slip velocity ratios in an air–water system under steady state and transient conditions. They proposed the following equation for the radial holdup profile

$$\varepsilon_G = \bar{\varepsilon} \left( \frac{n+2}{n} \right) \left( 1 - \left( \frac{r}{R} \right)^n \right) \quad (1)$$

where  $\bar{\varepsilon}$  is the radial chordal average gas holdup along the column diameter and the exponent  $n$  are parameters and  $\frac{r}{R}$  is the dimensionless radial position. The value of  $n$  is indicative of the steepness of the holdup profile. When  $n$  is large the profile is flat, for small  $n$  the profile is steep. The steepness of the holdup profile is reflected in the intensity of liquid circulation.

Later, Ueyama and Miyauchi [16] modified Eq. (1) as follows to include the possibility of finite gas holdup close to the wall

$$\varepsilon_G = \bar{\varepsilon} \left( \frac{n+2}{n} \right) \left( 1 - c \left( \frac{r}{R} \right)^n \right) \quad (2)$$

where  $c$  is an additional parameter which is indicative of the value of gas holdup near the wall. If  $c = 1$  there is zero holdup close to the wall, if  $c = 0$  holdup is constant with changing  $\frac{r}{R}$ .

More recently, Wu et al. [17] conducted research to study radial gas holdup profiles in bubble column reactors using air and water as the operating fluids, employing gamma ray Computed Tomography (CT). [17] used the following equation originally proposed by Luo and Svendsen [18] for the radial holdup profile

$$\varepsilon_G = \bar{\varepsilon} \left( \frac{n+2}{n+2-2c} \right) \left( 1 - c \left( \frac{r}{R} \right)^n \right) \quad (3)$$

Wu et al. [17] conducted correlation exercises to evaluate  $n$  and  $c$  based on the knowledge of the general operating variables and physical operating variables and physical properties of the system in order to estimate the gas holdup profile by Eq. (3). They concluded the following empirical relationships

$$n = 2.188 \times 10^3 \text{Re}_G^{-0.598} \text{Fr}_G^{0.146} \text{Mo}_L^{-0.004} \quad (4)$$

$$c = 4.32 \times 10^{-2} \text{Re}_G^{0.2492} \quad (5)$$

where

$$\text{Re}_G = \frac{DU_{SG}(\rho_L - \rho_G)}{\mu_L}, \text{Fr}_G = \frac{U_{SG}^2}{gD}, \text{Mo}_L = \frac{g\mu_L^4}{(\rho_L - \rho_G)\sigma_L^3} \quad (6)$$

$\bar{\varepsilon}_G$ , cross-sectional mean gas holdup was evaluated from the experimental data.

It is against these backgrounds that the present experimental work will investigate the multiphase flow phenomena observed on the transport of air–silicone oil mixtures in a vertical riser. Experimental studies have been conducted on a vertical 67 mm internal diameter vertical riser. A WMS was devised for air–silicone oil to measure cross-sectional void fraction and time averaged radial void fraction. The WMS is based on capacitance measurements and works with non-conductive materials such as silicone oil. Data obtained in these facilities was used for detailed analysis of phase distributions in a vertical riser in a quantitative manner. Real time monitoring of the two-phase flow behavior using a high speed video camera was also deployed to validate the prevailing flow patterns and void fraction distribution.

## 2. Overview of the experimental facility

All experiments were carried out on an inclinable pipe flow rig within the Engineering Laboratories of the Department of Chemical and Environmental Engineering at University of Nottingham. Details about the experimental apparatus have been previously reported Abdulkadir et al. [1], Abdulkadir et al. [19,20], Azzopardi et al. [21], Azzopardi [22], and Geraci et al. [23,24]. In brief, the experimental facility consists of a main test pipe section constructed from transparent acrylic glass. The 6 m test pipe section is of a 0.067 m internal diameter. The test pipe section may be rotated on the rig to allow it to incline between  $-5^\circ$  and  $90^\circ$  as shown in Fig. 1. For the experiments reported in this paper the rig test pipe section was mounted as a vertical riser.

The rig was charged with air–silicone oil mixture to study the flow regimes created by the circulation of various air–silicone oil mixtures created by the controlled pumped circulation of the oil from the reservoir and the compressed injection of air at the base of the inclined riser pipe. The resultant flow regimes created for the range of air–silicone oil injection circulation flow rates studied were recorded using wire mesh sensors (WMS) as shown in Fig. 2. This technology, described by Azzopardi et al. [2], Manera et al. [13] and Thiele et al. [25], can image the dielectric components in the pipe flow phases by measuring rapidly and continually the capacitances of the passing flow across several crossing points in the mesh.

### 2.1. High speed video system

A high speed video camera (Phantom, Fastcam-APX 120 K) with a resolution of  $512 \times 512$  pixels operating at 60,000 frames per second was used to visualize and validate the flow regimes identified during the experiments. The recording rate ranged from 150 to 1000 frames/s depending on the flow condition. Images were taken at a location of 4.5 m (67 pipe diameters) from the mixing section. This technique allowed capturing the image sequence of the flow. A white paper was placed on one side of the test section to reduce the effect of reflection of a beam of light on the recorded images.

## 3. Results and Discussion

### 3.1. Validation (testing) of WMS data

In order to validate the WMS data, the results are compared against electrical capacitance tomography (ECT) results. A detailed description of the theory behind the ECT technology according to Abdulkadir et al. [20] is described by Azzopardi et al. [21], Hammer [26], Huang [27] and Zhu et al. [28]. In this study, a ring of electrodes were placed around the circumference of the riser at a given height above the injection portals at the bottom of the 6 m riser section. This enabled the measurement of the instantaneous distribution of the flow phases over the cross-section of the pipe. The use of two such circumferential rings of sensor electrodes, located at a specified distance apart, enabled the determination of the rise velocity of any observed Taylor bubbles and liquid slugs. The twin-plane ECT sensors were placed at a distance of 4.4 and 4.489 m downstream of the air–silicone oil mixer located at the base of the riser.

In this study, the WMS measurement transducer was used to give detailed information about air–silicone oil flows whilst the ECT as a check on the void fraction measurement accuracy. It presents results of validation carried out to give ourselves confidence in the results presented by the instruments. Experimental measurements have been recorded with the aid of the above instrumentation at a liquid superficial velocity of 0.05–0.38 m/s and for

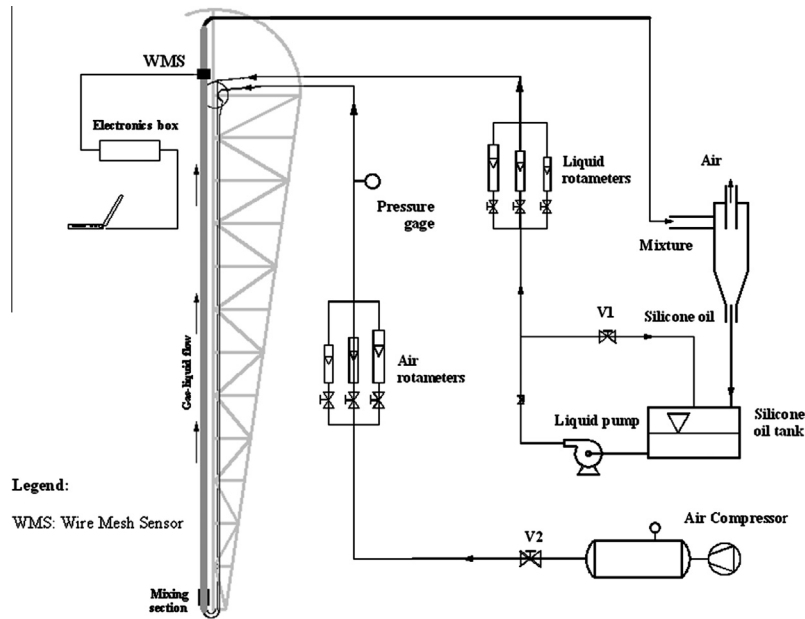


Fig. 1. Experimental facility employed in this work.

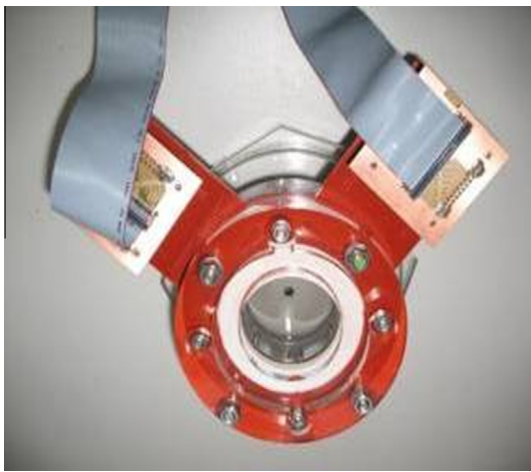


Fig. 2. Wire mesh sensor (WMS). Figure taken from Abdulkadir et al. [1].

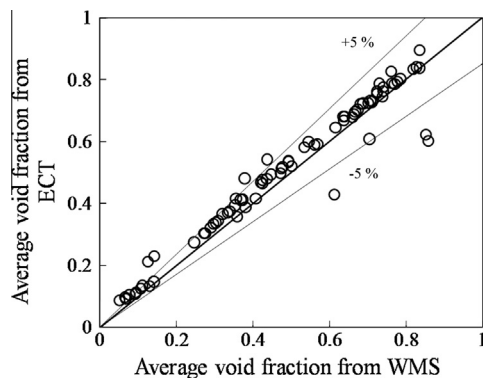


Fig. 3. Comparison between the average void fraction obtained from the WMS and ECT at a liquid superficial velocity of 0.05 m/s and gas superficial velocity of 0.05–4.73 m/s.

air flow rates in the range 0.05–4.73 m/s. The flow patterns covering these liquid and gas flow rates are spherical cap bubble, slug flow and churn flow as shown in Fig. 4. The electronics governing

the WMS measurement transducers was arranged to trigger the ECT transducer measurements to enable simultaneous recordings. The sampling frequencies of the ECT and WMS measurement transducers were 200 Hz and 1000 Hz, respectively. A great deal of information may be extracted from an examination of the time series of the cross-sectionally averaged void fractions. Fig. 3 shows the average void fraction recorded by the ECT and WMS measurement transducers. The observed difference between the results obtained by the ECT and WMS is within  $\pm 5\%$ . The data presented on the figure illustrates the good agreement between the two methods of measurements. Interestingly, Azzopardi et al. [29] also compared the output results of an ECT and WMS in a vertical pipe using air–silicone oil as the working fluid. They found good agreement. It is worth mentioning that for the WMS, the choice of permittivity model is not critical as the gap between the wires is small and is essentially either filled with liquid or gas. In this case, simple thresholding of the measurement is sufficient. On the other hand, the choice of physical model is critical for the ECT. Here, the capacitance measurement is converted to electrical permittivity using a Look-up Table Linearization from calibration at various permittivities.

### 3.2. Flow pattern map and test matrix

Fig. 4 shows the Shoham [30] flow pattern map generated for air/silicone oil with the operating points showing the various flow patterns obtained in the present study. It is worthy of mention that Fig. 5 is concerned with air/water flow. Both Figs. 4 and 5 are for upward flow in a vertical riser. The flow rates at which measurements were made for air–silicone oil flow are liquid and gas superficial velocities of (0.05–0.38) m/s and (0.05–4.74) m/s, respectively, whilst for air–water flow, the liquid superficial velocity is 0.25 m/s and gas superficial velocity is 0.05–2.83 m/s. It can be observed from Figs. 4 and 5 that slug flow is the most dominant flow pattern in this study.

### 3.3. Variation of time averaged cross-sectional void fraction distribution with gas superficial velocity

An interesting observation made here is that at a constant liquid superficial velocity, the void fraction changes drastically with the

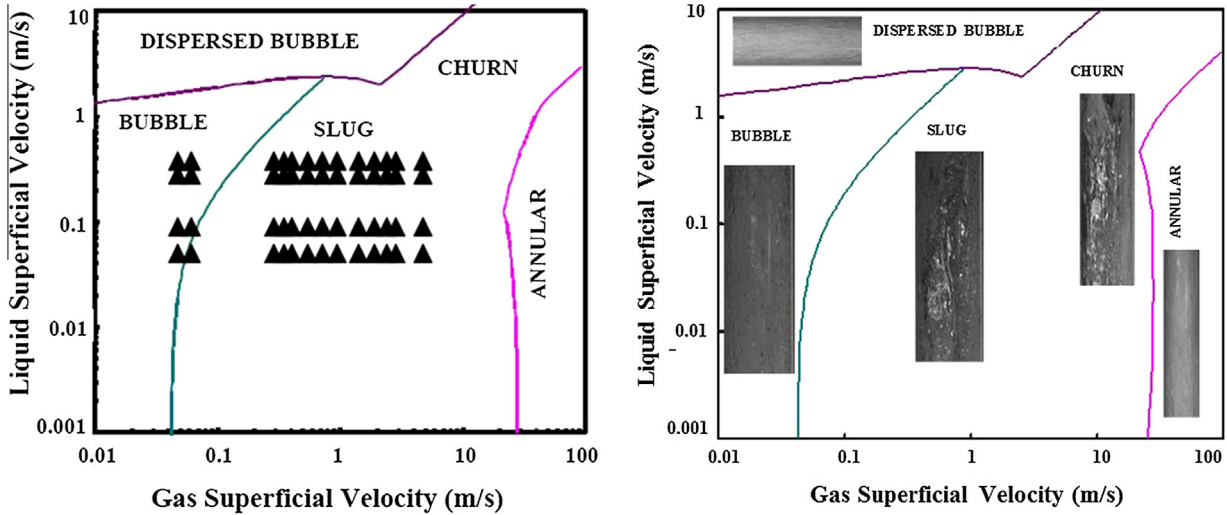


Fig. 4. Shoham [30]'s flow pattern map for vertical air/silicone oil flow.

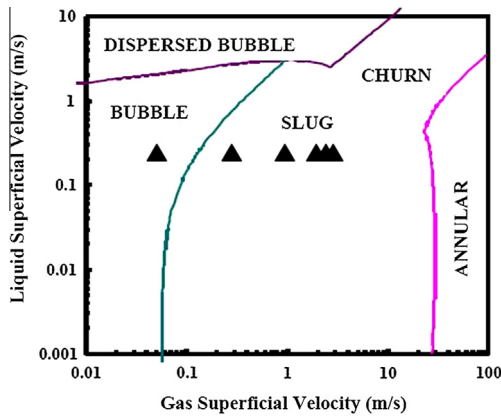


Fig. 5. Shoham [30]'s flow pattern map for vertical air/water oil flow.

prevailing flow patterns or on the other hand the gas superficial velocity. However, the average void fraction increases with a decrease in liquid superficial velocity. The variation of the void fraction at constant liquid superficial velocity and with increasing gas superficial velocity is presented in Fig. 6. Low void fraction values can be observed to be associated with spherical cap bubble ( $0.13 \leq \epsilon \leq 0.14$ ) and are seen to increase rapidly to slug flow ( $0.36 \leq \epsilon \leq 0.50$ ), unstable slug flow ( $\epsilon \leq 0.57$ ) and churn flow ( $0.66 \leq \epsilon \leq 0.83$ ) regimes with an increase in gas superficial velocity.

ity. Where  $\epsilon$  is average void fraction. This observed trend in void fraction is consistent with the observations of Bhagwat and Ghajar [31], Oshinowo and Charles [32] and Yijun and Rezkallah [33].

Fig. 6 can be observed to show that all the plots of average void fraction against gas superficial velocity followed the same trend. The plot shows that for a liquid superficial velocity of 0.05 m/s, the average void fraction, started initially with 0.1 at a gas superficial velocity of 0.05 m/s and extended to a maximum value of 0.80 at a gas superficial velocity of 4.7 m/s. It also shows that for liquid superficial velocities of 0.07, 0.09 and 0.14 m/s, the initial average void fraction is 0.1 at a gas superficial velocity of 0.05 m/s and reached same average void fraction of 0.8 at a gas superficial velocity of 4.7 m/s. For further liquid superficial velocities of 0.28 and 0.38 m/s, a least average void fraction of 0.80 is obtained at both gas superficial velocities of 4.7 m/s though starting with an average void fraction of 0.1 at a gas superficial velocity of 0.05 m/s. These observations suggest that the relationship between average void fraction and gas superficial velocity follows the trend  $\epsilon \propto U_{SG}^n$ , with the value of  $n$  depending on the degree of linearity. For  $n$  equals to 1, the relationship between  $\epsilon$  and  $U_{SG}$  is linear while for  $n$  less or greater than 1, non-linear. It can be observed that for almost all liquid superficial velocities, the relationship between average void fraction and gas superficial velocity is almost linear, with  $n \approx 1$  occurring within a region of gas superficial velocities of 0.05, 0.061 and 0.28 m/s. For an increase of gas superficial velocity from 0.28 to 2.8 m/s, the relationship deviates from

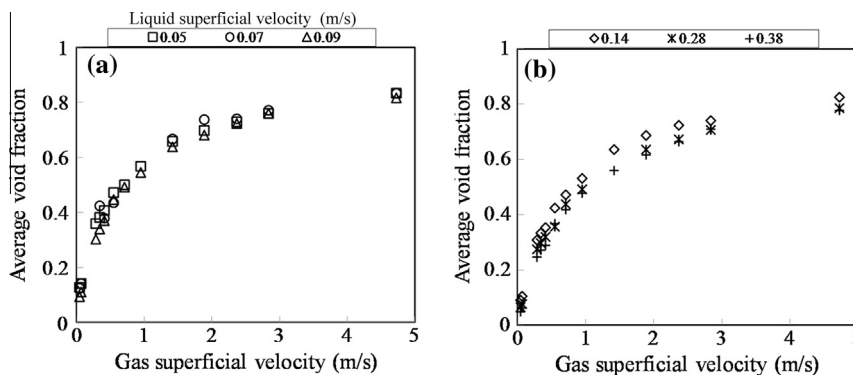


Fig. 6. Variation of time averaged cross-sectional void fraction with gas superficial velocity for different liquid superficial velocities of (a)  $0.05 < U_{SL} < 0.28$  m/s and (b)  $0.14 < U_{SL} < 0.38$  m/s.

linearity with  $n \approx 0.8$ . With a further increase of gas superficial velocity from 2.8 to 4.7 m/s, the trend is linear, with  $n \approx 1$ .

Figs. 7 and 8 support the observations made in Fig. 6 that as the liquid superficial velocity is maintained at 0.05 m/s and gas superficial velocity increased from 0.05 to 2.84 m/s, there are observed increases in average void fraction. This therefore maps the flow regime transition from spherical cap bubble to churn flow regimes.

3.4. Comparison of average void fraction from experimental data and empirical correlations

Here, the accuracy and consequently the performance of void fraction correlations will be carried out in terms of: (1) percentage error and (2) Root Mean Square (RMS) error. The performance analysis of the available correlations in order to select the best became necessary because most of the available correlations developed by different investigators were based on limited data, pipe diameter, flow pattern, fluid combinations and system pressure. The literature lacks a clear and universal definition of flow pattern and associated range of void fraction. Fig. 9 presents a comparison of the performance of average void fraction obtained from present study using WMS (experiment) and empirical correlations reported in literature based on percentage error. On the other hand, Fig. 10 depicts the comparison of the performance of average void fraction based on Root Mean Square (RMS) error.

The empirical correlations considered here are as follows: Morooka et al. [3], Bonnecaze et al. [34], and [35–47]. The error of deviation using the empirical correlations from experimental data is expressed in percentage. It can be concluded that the best correlation based on the percentage error method is the Kawanishi et al. [42] model with a  $\pm 10\%$  deviation.

The second method of selecting the best correlation based on the RMS error is carried out here. The RMS error is defined mathematically as:

$$RMS = \sqrt{\frac{1}{N-1} \sum_{i=1}^N \left( \frac{\alpha_{Predicted} - \alpha_{Measured}}{\alpha_{Measured}} \right)^2} \times 100\% \quad (7)$$

where  $N$  is the number of experimental data points

Eq. (7) was used to determine the RMS error and the obtained values are presented in Fig. 10. From Fig. 10, the Morooka et al. [3] correlation can be observed to have the least error of 9.6% as compared to the others. On the other hand, the Woldesemayat and Ghajar [46] Drift Flux model has the maximum error value of 50.6%.

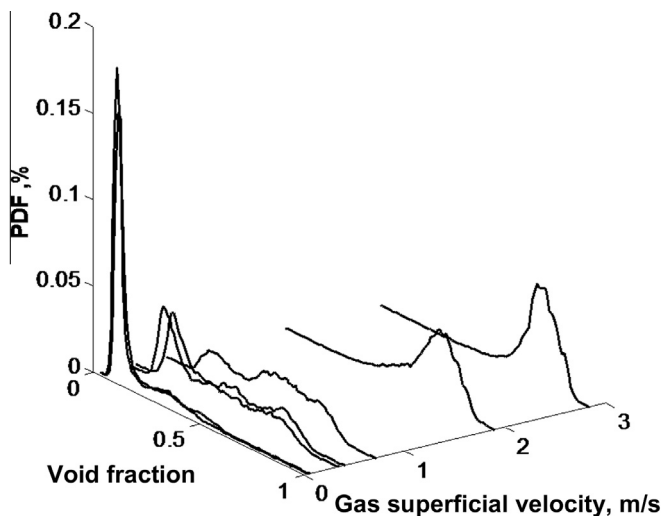


Fig. 7. 3-D probability density function (PDF) of void fraction measured by the WMS (liquid superficial velocity = 0.05 m/s and gas superficial velocity = 0.05–2.84 m/s).

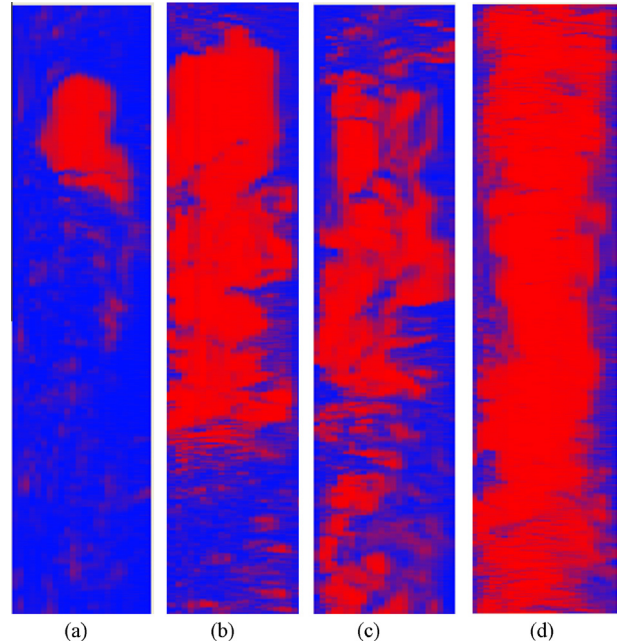


Fig. 8. Side view of the two-phase flow transition from spherical cap bubble to churn flow. Liquid superficial velocity of 0.05 m/s and gas superficial velocity of (a) 0.05 m/s (b) 0.7 m/s (c) 0.95 m/s and (d) 2.84 m/s. Sensor: wire mesh,  $24 \times 24$  sensitive points; time resolution: 1000 Hz.

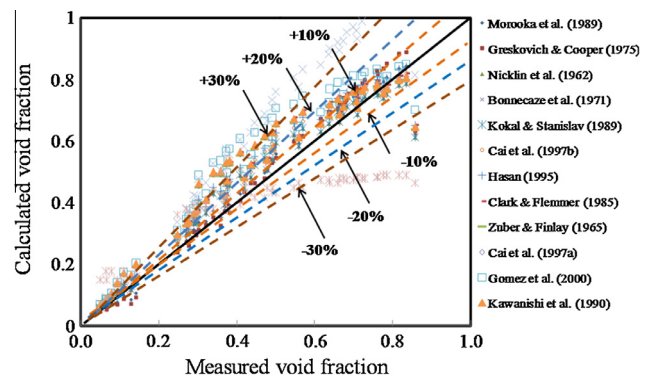


Fig. 9. Comparison of void fraction obtained using the WMS (present study) with empirical correlations.

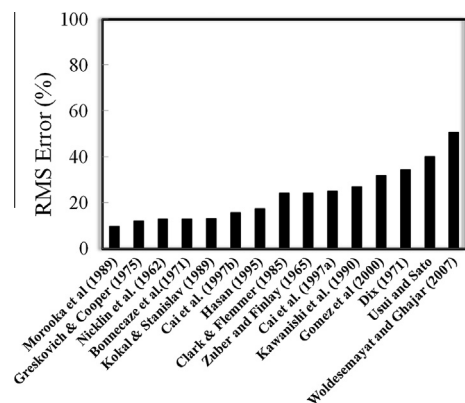


Fig. 10. Root Mean Square (RMS) error of average void fraction from empirical correlations.

3.5. Effect of gas superficial velocity on flow patterns and radial time averaged void fractions

The effect of gas superficial velocity on flow pattern and radial void fraction is presented and discussed here. This is shown in Fig. 11.

It can be observed from Fig. 11 that at liquid and gas superficial velocities of 0.05 m/s and  $0.05 < U_{SG} < 2.84$  m/s, respectively, parabolic profiles are obtained. The profiles show that maximum and minimum radial void fractions are observed at the center of the pipe and pipe wall respectively. The maximum radial void fractions for the six profiles as observed from the figure are 19.6%, 22.0%, 54.2%, 57.7%, 88.9%, and 94.6%, respectively. The profiles then moved downwards in a parabolic manner to a definite minimum. The minimum radial void fractions so obtained are 5.6%, 6.2%, 14.2%, 15.3%, 32.9% and 38.6% respectively. The maximum and minimum % radial void fractions occurred at 0.8 and 32.7 mm, respectively. The profiles obtained are in good agreement with the results reported by Ohnuki and Akimoto [12]. The results therefore, show that an increase in gas superficial velocity is responsible for an increase in radial void fraction at the center of the pipe and pipe wall. It is interesting to observe from the figure that at gas superficial velocities of 1.89 m/s and 2.84 m/s, the radial void fraction profiles started becoming flattened at the top as the gas superficial velocity increases, thus, giving an impression that the plots resembled turbulent flow profiles. The profiles obtained are in good agreement with the results obtained by Carver [48] and Carver and Salcudean [49] and Gardner and Neller [11] and contrary to the results obtained by [4]. The results show that the shape of the radial void fraction profile and an increase in percentage void fraction are dependent on gas superficial velocity as shown in Fig. 11.

Time varying void fraction data and probability density function (PDF) distributions are used to discriminate between the various flow patterns according to Costigan and Whalley [50] who defined a single peak PDF existing at low void fraction with a broadening tail as spherical cap bubble and twin peaked PDFs of recorded void fractions as slug flow. Also, that a PDF at high void fraction with a broadening tail down to low void fractions corresponds to churn flow. Following the PDF approach, Fig. 11 shows that the observed flow patterns are spherical cap bubble, slug and churn flows. However, the observed symmetric profiles can be classified as slug flow. The symmetric profiles, though with a flattened front as observed can be represented as churn flows.

3.6. Comparison between the radial void fraction for air–silicone oil and air–water

Here, a comparison between the data of air–water and air–silicone oil based on the radial void fraction distribution is presented in Fig. 12. The results show that a reasonably good trend is observed for both cases at same liquid superficial velocity but different gas superficial velocities.

It is interesting however, to observe from Fig. 12 that at gas superficial velocity of 0.05 m/s, there is a wide deviation between the values of the radial void fraction: at the center of the pipe, for air–silicone oil, 0.1 whilst for the air–water flow, 0.13; at the wall, 0.05 for the air–silicone oil and 0.008 for the air–water flow. The observed wide deviation in the void fraction could be attributed to the effect of fluid properties. The degree of agreement between the data for air–water and air–silicone oil improved with an increase in gas superficial velocity. This therefore, seems to suggest that at higher gas superficial velocities, the effect of fluid properties ceases to be an issue.

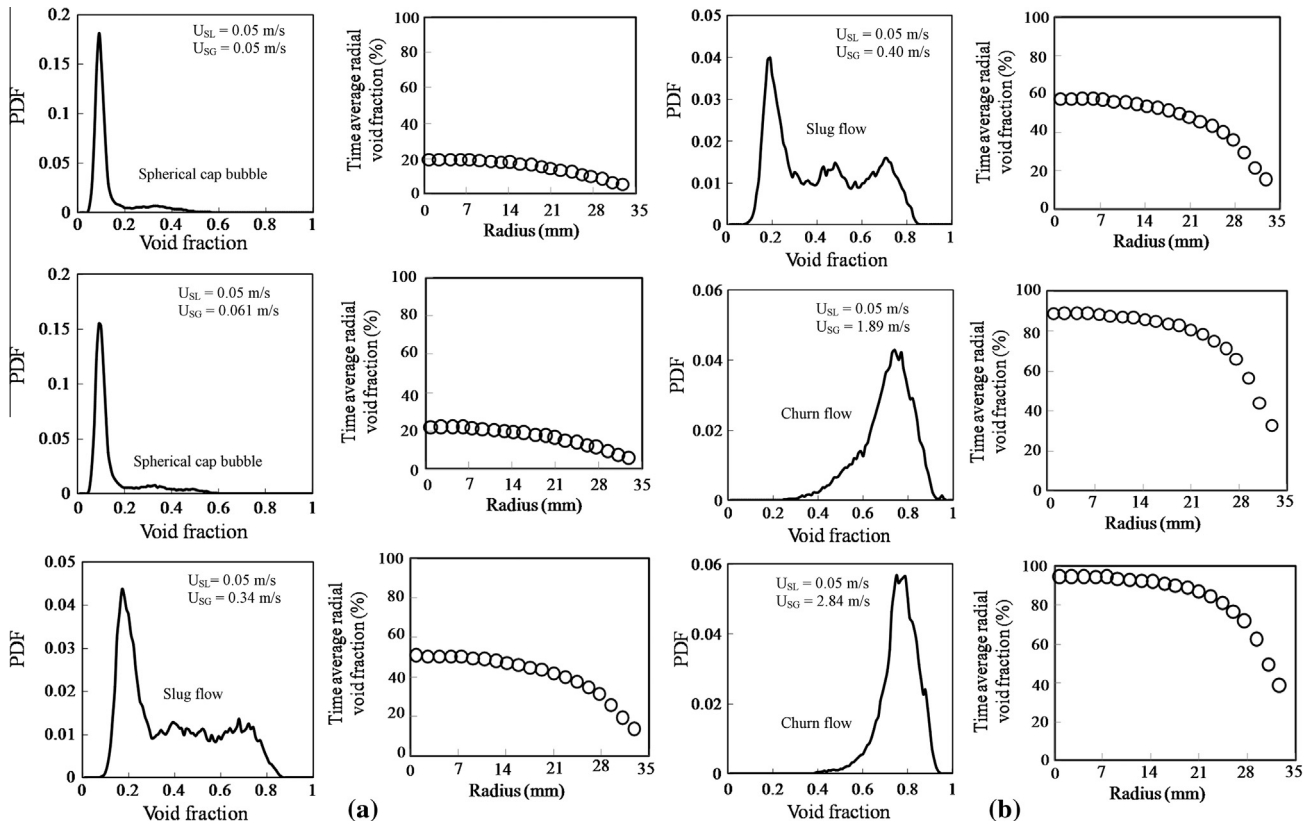


Fig. 11. The effect of gas superficial velocity on flow pattern and radial void fraction profile.

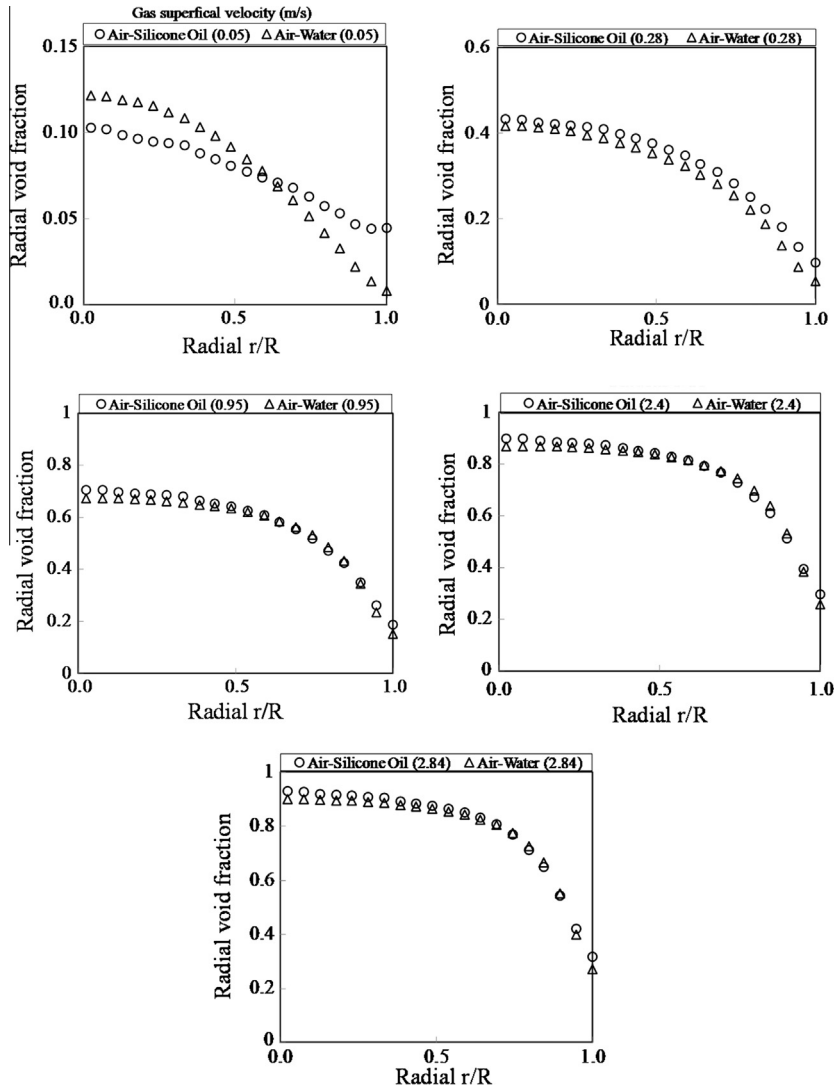


Fig. 12. Comparison of the radial void fraction for air–silicone oil and air–water at the same liquid superficial velocity of 0.25 m/s and different gas superficial velocities.  $r/R$  represents normalized pipe radius,  $r/R = 0.5$  represents center of the pipe radius,  $r/R = 1$  represents pipe wall and  $r/R = 0$  is the radius of the pipe.

3.7. Variation of  $c$ -parameter and steepness parameter with gas superficial velocity

The  $c$ -parameter as defined by Wu et al. [17] according to Eq. (5) is a parameter that defines the amount of gas near the wall. Here, the influence of increasing gas superficial velocity on  $c$ -parameter will be examined. The variation of steepness parameter with gas superficial velocity will also be examined. The plots of  $c$ -parameter and steepness parameter are presented in Figs. 13 and 14, respectively.

It can be observed from Fig. 13 that the  $c$ -parameter increases from 0.21 to 0.58 with an increase in gas superficial velocity. This means the amount of gas near the wall of the riser increases with an increase in gas superficial velocity.

The steepness parameter according to Wu et al. [17] based on Eq. (4) is used to define the sharpness of the void fraction or liquid holdup profile. From an analysis of the variation in steepness parameter with gas superficial velocity (Fig. 14), it is concluded that with an increase in gas superficial velocity the steepness parameter decreases from 23.4 to 6.7. This means that higher values of the steepness parameter could be used to represent spherical cap bubble, the intermediate values, slug flow, and the lower

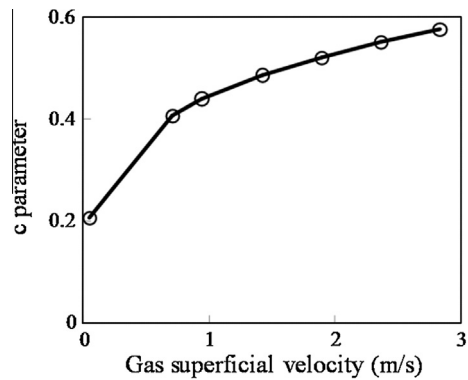


Fig. 13. Variation of  $c$ -parameter with gas superficial velocity. The  $c$ -parameter, Eq. (5) proposed by Wu et al. [17] was recalculated using the physical properties of air and silicone oil.

values, churn flow. This therefore shows that the variation of steepness parameter with gas superficial velocity may be used to classify the flow regimes present.



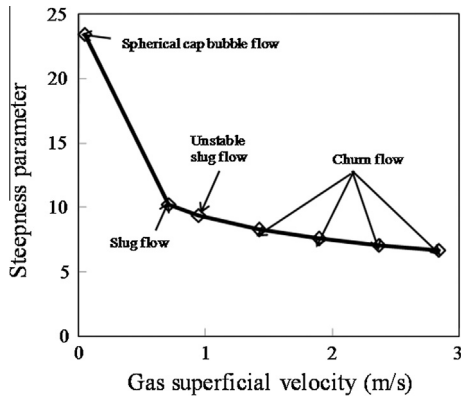


Fig. 14. Variation of steepness parameter with gas superficial velocity. The steepness parameter, Eq. (4) proposed by Wu et al. [17] was recalculated using the physical properties of air and silicone oil.

3.8. Comparison of experimental time averaged radial void fraction with Wu et al. [17]’s published Eq. (3)

The results of a comparative analysis of the experimental data with [17]’s published Eq. (3) is presented here.

From an examination of the experimental data plotted in Fig. 15, it is concluded that the radial void fraction increases with gas superficial velocity and that the shape of the profile is dependent on the gas superficial velocity.

It is interesting however, to note that contrary to the results obtained by [17] using Eq. (3), the profiles for bubble and slug flows are parabolic and semi-flat parabolic, respectively whilst for churn flow, flat parabolic as earlier reported by Abdulkadir et al. [1]. It can be observed that the Eq. (3) model is not suitable for replicating the observed radial void fraction at low gas superficial velocity.

The comparison between experiment and [17] published Eq. (3) is very poor at liquid and gas superficial velocities of 0.05 and 0.05 m/s, respectively as shown in Fig. 14a. The mean relative error is very high, 47.3%. The experiment predicts the profile as parabolic whilst the [17] published Eq. (3) as flat. The wide deviation could be as a result of this discrepancy.

For Fig. 15b–f, the radial void fraction presents a semi-flat parabolic profile. A better agreement is found for Fig. 15f, with a mean relative error of 5.7%. For slug flow (Fig. 15b and c) it has been found that the [17] published Eq. (3) under predicts and over predicts void fraction before and after the center of the radius of the pipe, respectively. The effects disappearing with an increase in gas superficial velocity for churn flow as shown in Fig. 15d–f. The

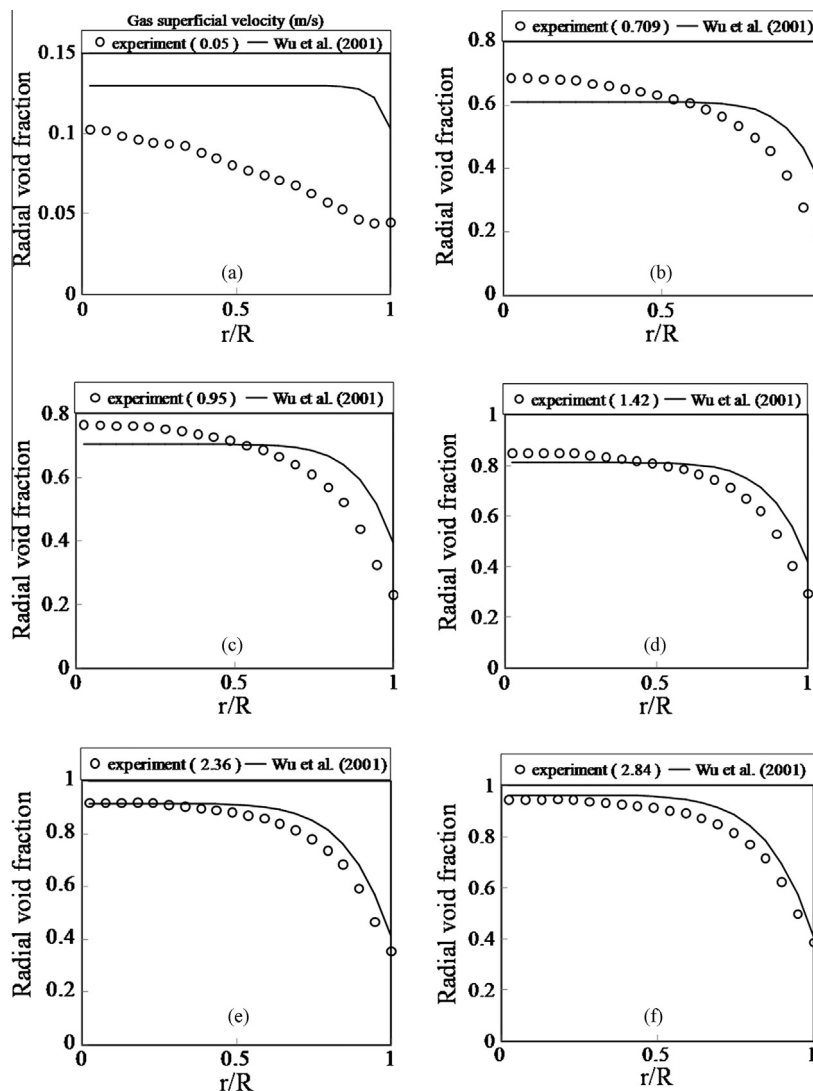


Fig. 15. Comparison of experimental time averaged radial void fraction distribution with [17]’s published equation at liquid and gas superficial velocities of 0.05 m/s and  $(0.05 < U_{SG} < 2.84 \text{ m/s})$ , respectively. The [17] published Eq. (3) was recalculated using the physical properties of air and silicone oil.

under prediction and over prediction of the void fraction could be due to the fact that the equation was originally developed for air–water systems.

#### 4. Conclusions

A detailed analysis of phase distribution in a vertical riser has been successfully carried out. Experiments were performed using an air/silicone oil mixture within a 6 m and 0.067 m internal diameter long riser. The air superficial velocities studied ranged from 0.05 to 4.74 m/s, whilst liquid superficial velocities ranged from 0.05 to 0.38 m/s. Measurements of the average cross-sectional and time average radial void fraction were obtained using a wire mesh sensor (WMS). The data were recorded at an acquisition frequency of 1000 Hz over an interval of 60 s. An analysis of the results show that:

The major flow patterns observed in the present study were found to be consistent with those reported in the literature.

At a constant liquid superficial velocity, the average cross-sectional void fraction changes drastically with the prevailing flow patterns or alternatively the gas superficial velocity.

The accuracy and hence the performance of the void fraction correlations was judged in terms of percentage error and RMS error. Based on these results and the outcome of the performance analysis of the correlations, Morooka et al. [3] is judged as the best performing correlation based on RMS error while on the other hand, Kawanishi et al. [42] the best based on percentage error.

The radial void fraction increases with gas superficial velocity and that the shape of the profile is dependent on gas superficial velocity. The profiles for cap/bubble, slug and churn flows are parabolic, semi-flat parabolic and flat parabolic profiles, respectively.

The data for air–water and air–silicone oil systems were reasonably similar except at gas superficial velocity of 0.05 m/s.

The steepness parameter decreases with an increase in gas superficial velocity whilst the *c*-parameter increases with an increase in gas superficial velocity. The steepness parameter can be used to classify flow regimes; high steepness values represent cap/bubble flow, intermediate values, slug flow and low values represent churn flow.

The Wu et al. [17] published Eq. (3) does not give satisfactorily replicating radial void fraction profile at low gas superficial velocities of our tests.

#### Acknowledgments

Abdulkadir, M., would like to express his sincere appreciation to the Nigerian government through the Petroleum Technology Development Fund (PTDF) for providing the funding for his doctoral studies.

This work has been undertaken within the Joint Project on Transient Multiphase Flows and Flow Assurance. The Author(s) wish to acknowledge the contributions made to this project by the UK Engineering and Physical Sciences Research Council (EPSRC) and the following: GL Industrial Services; BP Exploration; CD-adapco; Chevron; ConocoPhillips; ENI; ExxonMobil; FEESA; IFP; Institut for Energiteknikk; PDVSA (INTEVEP); Petrobras; PETRONAS; SPT; Shell; SINTEF; Statoil and TOTAL. The Author(s) wish to express their sincere gratitude for this support.

Special thanks go to Dr. Safa Sharaf for assisting in processing the wire mesh sensor (WMS) data.

#### References

- [1] M. Abdulkadir, V. Hernandez-Perez, S. Sharaf, I.S. Lowndes, B.J. Azzopardi, Experimental investigation of phase distributions of two-phase air–silicone oil flow in a vertical pipe, *World Acad. Sci. Eng. Technol. (WASET)* 61 (2010) 52–59.
- [2] B.J. Azzopardi, V. Hernandez-Perez, R. Kaji, M.J. da Silva, M. Beyer, U. Hampel, Wire mesh sensor studies in a vertical pipe, in: *HEAT 2008, Fifth International Conference on Multiphase Systems*, Bialystok, Poland, 2008.
- [3] S. Morooka, T. Ishizuka, M. Iizuka, K. Yoshimura, Experimental study on void fraction in a simulated BWR fuel assembly (evaluation of cross-sectional averaged void fraction), *Nucl. Eng. Des.* 114 (1989) 91–98.
- [4] A. Ohnuki, H. Akimoto, Experimental study on transition of flow pattern and phase distribution in upward air–water two-phase flow along a large vertical pipe, *Int. J. Multiphase Flow* 26 (3) (2000) 367–386.
- [5] H.-M. Prasser, E. Krepper, D. Lucas, Evolution of the two-phase flow in a vertical tube-decomposition of gas fraction profiles according to bubble size classes using wire mesh sensors, *Int. J. Therm. Sci.* 41 (2002) 17–28.
- [6] H.-M. Prasser, M. Misawa, I. Tiseanu, Comparison between wire-mesh sensor and ultra-fast X-ray tomograph for an air–water flow in a vertical pipe, *Flow Meas. Instrum.* 16 (2005) 73–83.
- [7] X. Shen, K. Mishima, H. Nakamura, Two-phase distribution in a vertical large diameter pipe, *Int. J. Heat Mass Transfer* 48 (2004) 211–225.
- [8] L. Szalinski, L.A. Abdulkareem, M.J. da Silva, S. Thiele, M. Beyer, D. Lucas, V. Hernandez-Perez, U. Hampel, B.J. Azzopardi, Comparative study of gas–oil and gas–water two-phase flow in a vertical pipe, *Chem. Eng. Sci.* 65 (2010) 3836–3848.
- [9] A.A. Harms, C.F. Forrest, Dynamic effects in radiation diagnosis of fluctuating voids, *Nucl. Sci. Eng.* 46 (1971) 408–413.
- [10] O.C. Jones, Determination of transient characteristics of an X-ray void measurement system for use in studies of two-phase flow, General Electric Co., Report, KAPL-3859, 1970.
- [11] G.C. Gardner, P.H. Neller, Phase distributions flow of an air–water mixture round bends and past obstructions, *Proc. Inst. Mech. Eng.* 184 (3C) (1969) 93–101.
- [12] A. Ohnuki, H. Akimoto, An experimental study on developing air–water two-phase flow along a large vertical pipe: effect of air injection method, *Int. J. Multiphase Flow* 22 (6) (1996) 143–1154.
- [13] A. Manera, B. Ozar, S. Paranjape, M. Ishii, H.-M. Prasser, Comparison between wire-mesh-sensors and conducting needle-probes for measurements of two-phase flow parameters, *Nucl. Eng. Des.* 239 (2008) 1718–1724.
- [14] G.B. Wallis, *One-dimensional two-phase flow*, second ed., McGraw Hill, New York, 1969.
- [15] G.P. Nassos, S.G. Bankoff, Slip velocity ratios in an air–water system under steady-state and transient conditions, *Chem. Eng. Sci.* 22 (667) (1967) 661–668.
- [16] K. Ueyama, T. Miyauchi, Properties and recirculating turbulent two-phase flow in gas bubble columns, *AIChE J.* 25 (1979) 298.
- [17] Y. Wu, B. Cheng Ong, M.H. Al-Dahhan, Predictions of radial gas holdup in bubble column reactors, *Chem. Eng. Sci.* 56 (2001) 1207–1210.
- [18] H. Luo, H.F. Svendsen, Turbulent circulation in bubble columns from eddy viscosity distributions of single-phase pipe flow, *Can. J. Chem. Eng.* 69 (1991) 1389–1394.
- [19] M. Abdulkadir, V. Hernandez-Perez, I.S. Lowndes, B.J. Azzopardi, Experimental study of the hydrodynamic behaviour of slug flow in a vertical riser, *Chem. Eng. Sci.* 106 (2014) 60–75.
- [20] M. Abdulkadir, D. Zhao, L. Abdulkareem, S. Sharaf, I.S. Lowndes, B.J. Azzopardi, Interrogating the effect of 90° bends on air–silicone oil flows using advanced instrumentation, *Chem. Eng. Sci.* 66 (2011) 2453–2467.
- [21] B.J. Azzopardi, L. Abdulkareem, S. Sharaf, M. Abdulkadir, V. Hernandez-Perez, A. Ijoma, Using tomography to interrogate gas–liquid flow, in: *28th UIT Heat Transfer Congress*, Brescia, Italy, 2010, 21–23 June.
- [22] B.J. Azzopardi, Drops in annular two-phase flow, *Int. J. Multiphase Flow* 23 (1997) 1–53.
- [23] G. Geraci, B.J. Azzopardi, H.R.E. Van Maanen, Inclination effects on circumferential film distribution in annular gas/liquid flows, *AIChE J.* 53 (2007) 1144–1150.
- [24] G. Geraci, B.J. Azzopardi, H.R.E. Van Maanen, Effects of inclination on circumferential film thickness variation in annular gas/liquid flows, *Chem. Eng. Sci.* 62 (2007) 3032–3042.
- [25] S. Thiele, M.J. da Silva, U. Hampel, L.A. Abdulkareem, B.J. Azzopardi, High-resolution oil–gas two-phase flow measurement with a new capacitance wire-mesh tomography, in: *5th Int. Symp. on Proc. Tomography*, Poland, Zakopane, 25–26 August, 2008.
- [26] E.A. Hammer, *Three-component Flow Measurement in Oil/Gas/Water Mixtures Using Capacitance Transducers*, PhD thesis, University of Manchester, 1983.
- [27] S.M. Huang, Impedance sensors-dielectric systems, in: R.A. Williams, M.S. Beck (Eds.), *Process Tomography*, Butterworth-Heinemann Ltd., Cornwall, 1995.
- [28] K. Zhu, R.S. Madhusudana, C. Wang, S. Sundaresan, Electrical capacitance tomography measurements on vertical and inclined pneumatic conveying of granular solids, *Chem. Eng. Sci.* 58 (2003) 4225–4245.
- [29] B.J. Azzopardi, L.A. Abdulkareem, D. Zhao, S. Thiele, M.J. da Silva, M. Beyer, A. Hunt, Comparison between electrical capacitance tomography and wire mesh sensor output for air/silicone oil flow in a vertical pipe, *Ind. Eng. Chem. Res.* 49 (2010) 8805–8811.
- [30] O. Shoham, *Mechanistic Modelling of Gas–Liquid Two-phase Flow in Pipes*, University of Tulsa, Society of Petroleum Engineers, USA, 2006.
- [31] S.M. Bhagwat, A.J. Ghajar, Similarities and differences in the flow patterns and void fraction in vertical upward and downward two phase flow, *Exp. Therm. Fluid Sci.* 39 (2012) 213–227.

- [32] T. Oshinowo, M.E. Charles, Vertical two-phase flow – Part 1: Flow pattern correlations, *Can. J. Chem. Eng.* 52 (1974) 25–35.
- [33] J. Yijun, K. Rezkallah, A study on void fraction in vertical co-current upward and downward two-phase gas–liquid flow – 1: experimental results, *Chem. Eng. Commun.* 126 (1993) 221–243.
- [34] R.H. Bonnecaze, W. Erskine, E.J. Greskovich, Hold up and pressure drop for two phase slug flow in inclined pipelines, *AIChE* 17 (1971) 1109–1113.
- [35] J. Cai, T. Chen, Q. Ye, Void fraction in bubbly and slug flow in downward air–oil two phase flow in vertical tubes, in: *International Symposium on Multiphase Flow*, Beijing, 1997a.
- [36] J. Cai, T. Chen, Q. Ye, Void fraction in bubbly and slug flow in downward air–oil two phase flow in vertical tubes, in: *International Symposium on Multiphase Flow*, Beijing, 1997b.
- [37] N.N. Clark, R.L. Flemmer, Predicting the holdup in two-phase bubble upflow and downflow using the Zuber and Findlay Drift Flux model, *AIChE* 31 (3) (1985) 500–503.
- [38] G.E. Dix, Vapour Void Fractions for Forced Convection with Sub cooled Boiling at Low Flow Rates, Ph.D. thesis, University of California, Berkeley, 1971.
- [39] L.E. Gomez, O. Shoham, Z. Schmidt, R.N. Chokshi, T. Northug, Unified mechanistic model for steady-state two-phase flow: horizontal to vertical upward flow, *Soc. Petrol. Eng. J.* 5 (3) (2000) 339–350.
- [40] E.J. Greskovich, W.T. Cooper, Correlation and prediction of gas–liquid holdups in inclined upflows, *AIChE J.* 21 (1975) 1189–1192.
- [41] A.R. Hasan, Void fraction in bubbly and slug flow in downward vertical and inclined systems, *Soc. Petrol. Eng. Prod. Facil.* 10 (3) (1995) 172–176.
- [42] K. Kawanishi, Y. Hirao, A. Tsuge, An experimental study on drift flux parameters for two-phase flow in vertical round tubes, *Nucl. Eng. Des.* 120 (1990) 447–458.
- [43] S.L. Kokal, J.F. Stainslav, An experimental study of two phase flow in slightly inclined pipes II: liquid holdup and pressure drop, *Chem. Eng. Sci.* 44 (1989) 681–693.
- [44] D.J. Nicklin, J.O. Wilkes, J.F. Davidson, Two-phase flow in vertical tubes, *Trans. Inst. Chem. Eng.* 40 (1962) 61–68.
- [45] K. Usui, K. Sato, Vertically downward two-phase flow (1) void distribution and average void fraction, *J. Nucl. Sci. Technol.* 26 (1989) 670–680.
- [46] M.A. Woldesemayat, A.J. Ghajar, Comparison of void fraction correlations for different flow patterns in horizontal and upward inclined pipes, *Int. J. Multiphase Flow* 33 (2007) 347–357.
- [47] N. Zuber, J.A. Findlay, Average volumetric concentration in two-phase flow systems, *J. Heat Transfer* 87 (1965) 453–468.
- [48] M.B. Carver, Numerical computation of phase separation in two fluid flow, *ASME Paper*, 106/153 (82-FE-2), 1984.
- [49] M.B. Carver, M. Salcudean, Three-dimensional numerical modelling of phase distribution of two-fluid flow in elbows and return bends, *Numer. Heat Transfer* 10 (1986) 229–251.
- [50] G. Costigan, P.B. Whalley, Slug flow regime identification from dynamic void fraction measurements in vertical air–water flows, *Int. J. Multiphase Flow* 23 (1997) 263–282.